Journal of Alloys and Compounds 509 (2011) 9372–9376

Contents lists available at ScienceDirect

Journal of Alloys and Compounds

journal homepage: www.elsevier.com/locate/jallcom

# Decorating Mg/Fe oxide nanotubes with nitrogen-doped carbon nanotubes

Yong Cao[a,*], Qingze Jiao[b,**], Yun Zhao[b], Yingchao Dong[c]

[a] Institute of Environment and Municipal Engineering, North China Institute of Water Conservancy and Hydroelectric Power, Zhengzhou 450011, PR China
[b] School of Chemical Engineering and the Environment, Beijing Institute of Technology, Beijing 100081, PR China
[c] Materials and Surface Science Institute (MSSI), University of Limerick, Limerick, Ireland

ARTICLE INFO

*Article history:*
Received 21 May 2011
Received in revised form 12 July 2011
Accepted 14 July 2011
Available online 23 July 2011

*Keywords:*
Oxide nanotubes
Nitrogen-doped carbon nanotubes
Magnetic property

ABSTRACT

Mg/Fe oxide nanotubes decorated with nitrogen-doped carbon nanotubes ($CN_x$) were fabricated by catalytic chemical vapor deposition of ethylenediamine on the outer surface of oxide nanotubes. Mg/Fe oxide nanotubes were prepared using a 3:1 molar precursor solution of $Mg(NO_3)_2$ and $Fe(NO_3)_3$ and anodic aluminum oxide as the substrate. The obtained samples were characterized by X-ray diffraction (XRD), transmission electron microscopy (TEM), scanning electron microscopy (SEM), X-ray photoelectron spectroscopy (XPS) and vibrating sample magnetometer (VSM). The XRD pattern shows that the oxide nanotubes are made up of MgO and $Fe_2O_3$. TEM and SEM observations indicate the oxide nanotubes are arrayed roughly parallel to each other, and the outer surface of oxide nanotubes are decorated with $CN_x$. XPS results show the nitrogen-doped level in $CN_x$ is about 7.3 at.%. Magnetic measurements with VSM demonstrate the saturated magnetization, remanence and coercivity of oxide nanotubes are obvious improved after being decorated with $CN_x$.



## 1. Introduction

Carbon nanotubes (CNTs) have been the focus of intensive study for their unique structural, electrical, and mechanical properties since their discovery by Iijima [1]. Their potential applications include nanodevices, quantum wires, ultrahigh-strength engineering fibers, sensors, and catalyst supports [2–4]. The doping of CNTs with nitrogen atoms is an effective way to tailor the electrical properties of CNTs. The additional electrons contributed by the N-doping provide electron carriers for the conduction band [5], which makes the N-doped CNTs ($CN_x$) either metallic or semiconductive with a narrow energy gap [6], thus offering the possibility of greater electrical conductivity than the pure CNTs.

Inspired by the discovery of CNTs, extensive research efforts have been devoted to tubular nanostructures. Various nanotubes, such as sulfides, nitrides, metals and oxides [7–10], have been synthesized in template matrices. Compared with other nanostructures, nanotubes possess low mass density, high porosity and increased surface area [11], which are especially important in applications involving interactions between gases or liquids and the surface of a material [12]. These nanotubes have made important contributions to fundamental research in the areas of catalysis [13], sensors [14], electronic or magnetic devices [15,16], and biological separation and transport [17].

To optimize the uses of nanotubes in many fields, it is necessary to decorate the surface of nanotubes. For example, decorating can improve dispersion of CNTs in solvents or impart new optical, electric, magnetic properties [18–20]. Recently, decorating CNTs with different materials, such as magnetic nanoparticles [21–23], noble metals [24–26], polymers [27–29] and biomaterials [30,31] have been extensively reported. However, there are few reports about decorating oxide nanotubes. In our previous work, Zn/Co/Fe oxide nanotubes [32] and $CN_x$ [33] had been successfully prepared. Especially, $CN_x$ were prepared with Mg/Fe oxides obtained from layered double hydroxides as catalysts. Basing on those works, we grow $CN_x$ on the outer surface of Mg/Fe oxide nanotubes to obtain the decorated oxide nanotubes in this manuscript. We expect the decorated oxide nanotubes not only possess the excellent magnetic properties of magnetic oxide nanotubes, but also possess the greater electrical conductivity derived from $CN_x$.

## 2. Experimental

### 2.1. Preparation of Mg/Fe oxide nanotubes

Anodic aluminum oxide (AAO) membrane (Whatman, Anodisc 47, 200 nm) was commercially obtained and used as received. The precursor solution was prepared by dissolving $Mg(NO_3)_2$ and $Fe(NO_3)_3$ with a molar ratio of 3:1 (Mg:Fe = 3:1) in distilled water to form an aqueous solution of nitrate. Then the AAO template was immersed into the precursor solution for about 24 h at room temperature. Subsequently, the AAO template was put under vacuum at room temperature for 4 h and then dried at 100 °C for 4 h. After that, the template was heated at 500 °C for 1 h

* Corresponding author. Tel.: +86 371 69127436; fax: +86 371 69127436.
** Corresponding author. Tel.: +86 10 68918979; fax: +86 10 68918979.
*E-mail addresses:* caoyangel@126.com (Y. Cao), jiaoqz@bit.edu.cn (Q. Jiao).

0925-8388/$ – see front matter © 2011 Elsevier B.V. All rights reserved.
doi:10.1016/j.jallcom.2011.07.039

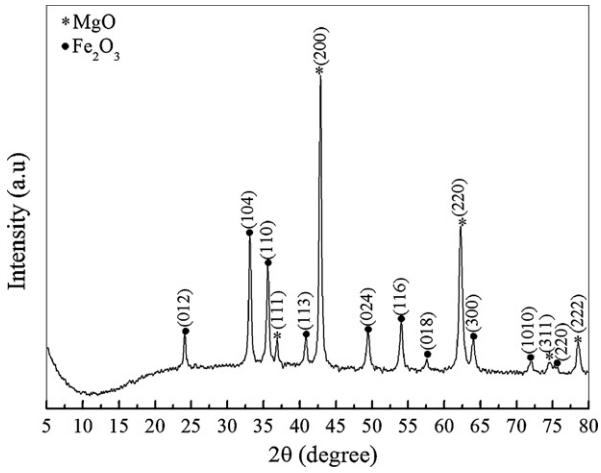


**Fig. 1.** XRD pattern of Mg/Fe oxide nanotubes.

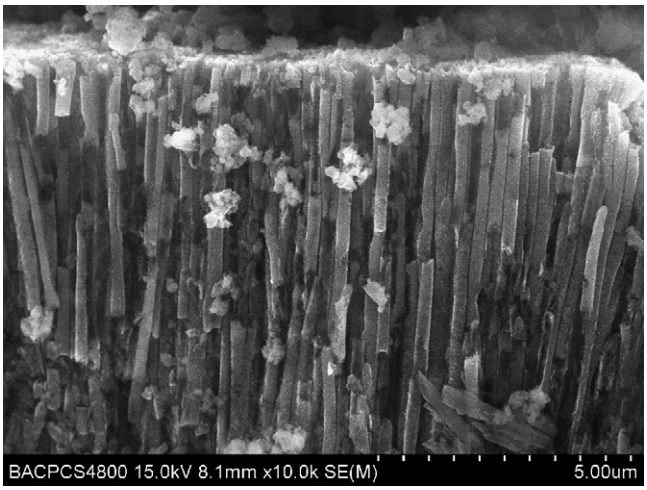


**Fig. 2.** SEM images of Mg/Fe oxide nanotube arrays.

in air, at a heating rate of 1 °C/min, and arrays of Mg/Fe oxide nanotubes inside the AAO templates were obtained. To remove the AAO template, they were then immersed in a 3 mol/L NaOH solution for 40 min at room temperature. Finally, after being washed with distilled water and dried at 100 °C for 2 h, one-dimensional Mg/Fe oxide nanotube arrays were obtained.

### 2.2. Preparation of Mg/Fe oxide nanotubes decorated with $CN_x$

About 20 mg of Mg/Fe oxide nanotubes were loaded in a quartz boat and placed in the middle of a tube furnace, which was heated under a flowing Ar (200 $cm^3$/min) at a rate of 1 °C/min. Between 350 and 400 °C, Ar was switched to $H_2$ (120 $cm^3$/min). On reaching 580 °C, ethylenediamine was pumped into the furnace at a rate of 0.15 $cm^3$/min with flow of Ar (400 $cm^3$/min). The reaction was maintained for about 20 min, after which the furnace was allowed to cool down to room temperature under Ar. Then the Mg/Fe oxide nanotubes decorated with $CN_x$ were obtained.

### 2.3. Characterization

The X-ray powder diffraction (XRD) of oxide nanotubes was collected on an X'pert PRO MPD diffractometer operated at 40 kV and 40 mA with Cu Kα radiation. The morphologies of oxide nanotubes were observed through transmission electron microscopy (TEM) with a JEOL JEM-1200EX instrument operated at 100 kV. Field emission scanning electron microscopy (FE-SEM) was performed by using a

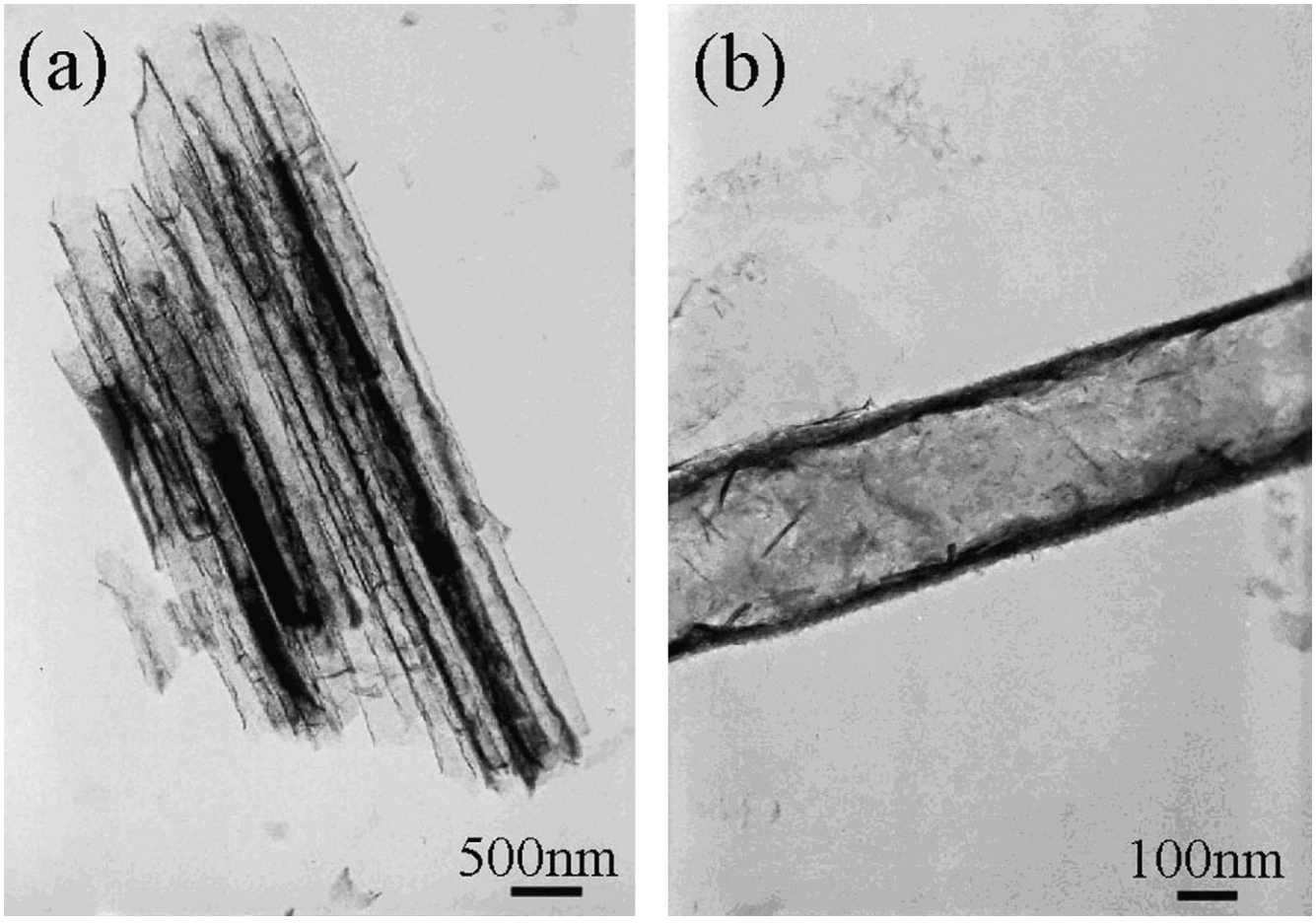


**Fig. 3.** TEM images of Mg/Fe oxide nanotubes.

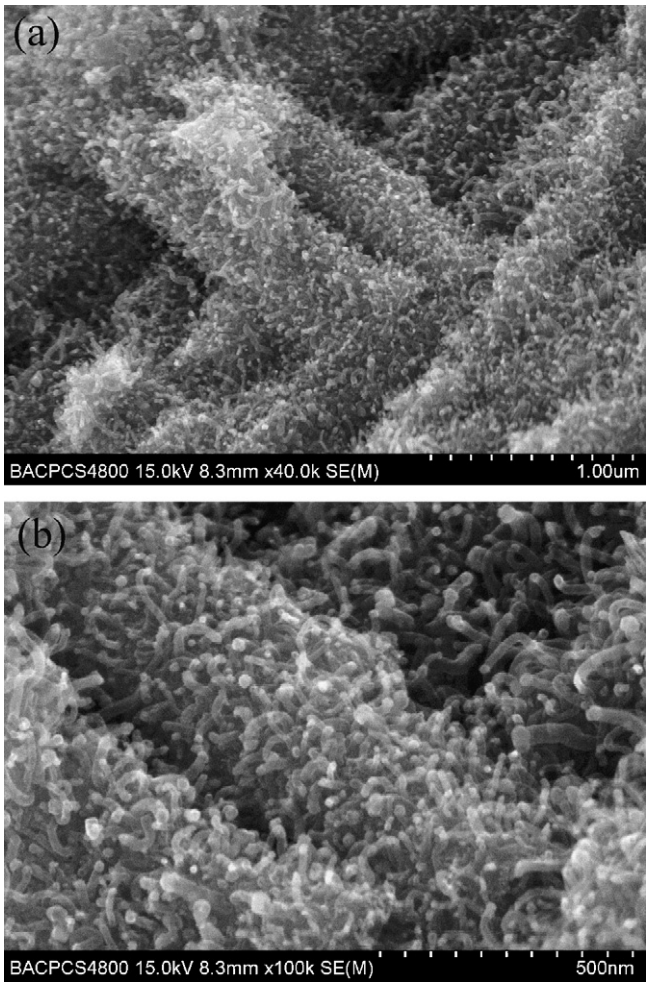


**Fig. 4.** SEM images of the Mg/Fe oxide nanotubes decorated with $CN_x$.

Hitachi S-4800 microscope operated at 15 kV. The N-doped level and the structure of N in $CN_x$ were determined by X-ray photoelectron spectroscopy (XPS, Physical electronics PHI 5300) using a vacuum generators XPS system operating with Mg (Kα) radiation. The raw data was corrected for charging using the binding energy of graphite at 284.6 eV. Peak areas were determined after back ground subtraction using Shirley's method and fitting the spectra with Gaussian curves. The content of N incorporated was calculated from the peak areas of the C1s and N1s peaks after being corrected for differences in sensitivity using sensitivity factors of 0.25 and 0.42 for C and N, respectively. The magnetic properties of the decorated oxide nanotubes were measured using a vibrating sample magnetometer (VSM) with a Lake Shore 7407 instrument. The samples were measured under a magnetic field of 12 kOe at room temperature.

## 3. Results and discussion

Fig. 1 shows the XRD pattern of the oxide nanotubes. The reflections indicate that the oxide nanotubes are the mixture of MgO (JCPDS, No. 75-0447) and $Fe_2O_3$ (JCPDS, No. 84-0307). It means that all $Mg(NO_3)_2$ and $Fe(NO_3)_3$ are transformed to the corresponding MgO and $Fe_2O_3$ after being calcinated at 500 °C. There is no obvious peak at about $2\theta = 30°$, which indicates the spinel phase $MgFe_2O_4$ (JCPDS, No. 01-1120) cannot be obtained under this condition. This result is different with our previous work, in which the spinel phase $MgFe_2O_4$ is obtained due to the particular structure of layered double hydroxide precursor [33].

Fig. 2 shows the FE-SEM images of Mg/Fe oxide nanotube arrays without AAO template. It is found that the nanotubes are roughly parallel to each other orderly and uniformly. The outer diameter of these nanotubes, limited by the size of channels in AAO template, is about 200 nm. The length of these nanotubes is not very uniform; a lot of long and short nanotubes are coexisted in our products. In addition to the tubular structure, there are also some large particles. These short nanotubes and particles may be formed owing to the destroyed long nanotubes during the high temperature calcined course.

TEM images of Mg/Fe oxide nanotubes are shown in Fig. 3. These nanotubes with an uneven length are roughly parallel to each other orderly (Fig. 3(a)), which is consistent with the SEM image in Fig. 2. From Fig. 3(b), the thickness of the oxide nanotubes wall is about 30 nm. For the ends of nanotubes, almost all oxide nanotubes are opened whereas CNTs are always closed. This phenomenon can be explained by the growth mechanism for both nanotubes. As we all known, CNTs are usually grown from the bottom or top where catalysts locate [34]. The growth of oxide nanotubes can be described as follows: firstly, capillary force and wetting ability of the aqueous solution make the pore of AAO template filled with nitrates solution. Owning to the attraction between the wall of AAO and the nitrates [35,36], the nanotubes made up of $Mg(NO_3)_2$ and $Fe(NO_3)_3$ are formed after being dried at room temperature under vacuum and at 100 °C in air. Finally, the oxide nanotubes composed by MgO and $Fe_2O_3$ are obtained after being calcined at 500 °C and AAO template is removed. So it is easy to understand why the ends of oxide nanotubes are opened.

SEM images of the Mg/Fe oxide nanotubes decorated with $CN_x$ are shown in Fig. 4. The outer surfaces of oxide nanotubes are wrapped tightly by $CN_x$, which confirms the decorating of oxide nanotubes with $CN_x$ has been realized. This process can be described as follows: when the temperature of the quartz boat loaded oxide nanotubes increases to 350 °C, the $Fe_2O_3$ lain on the outer surface of nanotubes can be reduced to Fe nanoparticles in $H_2$ atmosphere, whereas MgO is retained [33]. On reaching 580 °C, the Fe nanoparticles are acted as active centers to grow $CN_x$ when C

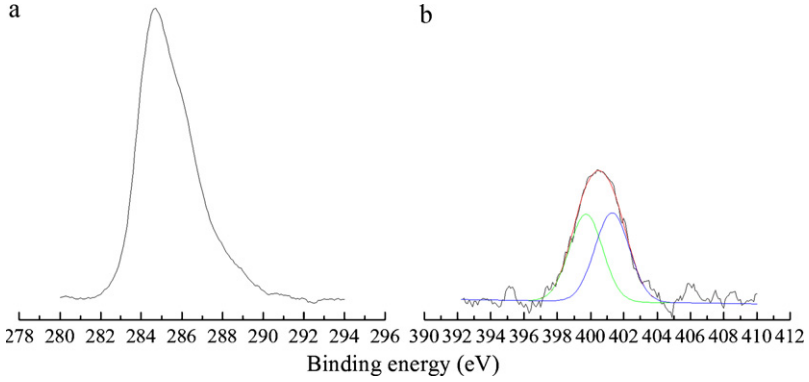


**Fig. 5.** C1s (a) and N1s (b) XPS spectra of $CN_x$.

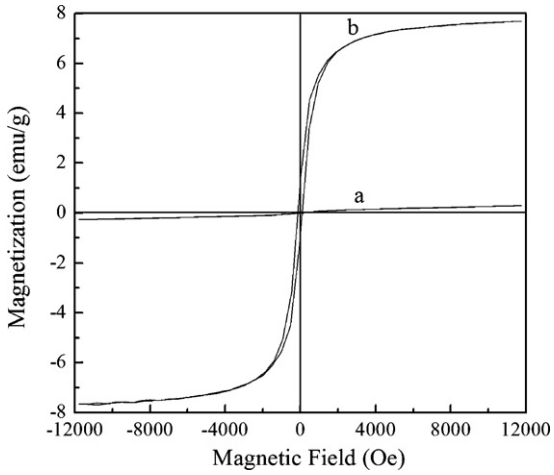


**Fig. 6.** Magnetization curves of Mg/Fe oxide nanotubes before (a) and after (b) being decorated.

**Table 1**
The magnetic properties of the samples.

| Samples | Hc (Oe) | Ms (emu/g) | Mr (emu/g) |
|---|---|---|---|
| Mg/Fe oxide nanotubes | 50.55 | 0.28 | 0.004 |
| Mg/Fe oxide nanotubes decorated with $CN_x$ | 110.81 | 7.70 | 1.06 |

and N atoms adsorb on them. As shown in Fig. 4(a), the diameter of the decorated oxide nanotubes is about 400–500 nm. Deducted the diameter of oxide nanotubes (200 nm), the length of $CN_x$ is about 100–150 nm. The diameter of $CN_x$ is about 15–30 nm. From Fig. 4(b), many nanoparticles encapsulated at the tips of $CN_x$ can be observed, which confirms these $CN_x$ following a tip-growth mechanism [34].

XPS analysis is carried out on $CN_x$ to investigate the level and structure of N. The C1s and N1s XPS spectra of $CN_x$ are displayed in Fig. 5(a and b), respectively. The asymmetric C1s band and N1s band can be observed centered at 284.6 eV and 400.4 eV. All XPS spectra show that the tubes consist of C accompanied by traces of N. The N-doped level of our product is about 7.3 at.%. From the curve fitting, the N1s band can be deconvoluted into two bands at around 399.7 eV (PN1) and 401.4 eV (PN2). The PN1 and PN2 correspond to pyridine-like and graphitic-like N [37,38]. The pyridine-like N is referred to the N atoms that contribute to the system with a pair of pi electrons, whereas graphitic-like N corresponds to the coordinated N atoms substituting for C atoms in the graphite layer [39]. The intensity of PN1 and PN2 is about 49% and 51%, which means that both structures have a similar content in our products.

The magnetic properties of the decorated Mg/Fe oxide nanotubes were measured in fields between ±12 kOe at room temperature. The hysteresis loops of oxide nanotubes before and after being decorated are presented in Fig. 6. Their magnetic parameters are summarized in Table 1. The hysteresis loops of the decorated oxide nanotubes (Fig. 6(b)) exhibits a typical ferromagnetic behavior. It can be seen that the coercivity (Hc), saturated magnetization (Ms) and remanence (Mr) of the decorated oxide nanotubes are largely increased. The reason may be attributed to the $Fe_2O_3$ phase within oxide nanotubes being reduced to Fe nanoparticles.

## 4. Conclusions

The Mg/Fe oxide nanotubes decorated with $CN_x$ were prepared successfully by catalytic chemical vapor deposition of ethylenediamine on the outer surface of oxide nanotubes at 580 °C. The reduced Fe nanoparticles acted as active centers. Mg/Fe oxide nanotubes, with an uneven length and roughly parallel to each other, were obtained via a template method. The $CN_x$ used to decorate have a diameter and length of about 15–30 nm and 100–150 nm, respectively. The N-doped level of $CN_x$ is about 7.3 at.%. After being decorated, oxide nanotubes exhibit ferromagnetic properties with the coercivity, saturated magnetization and remanence are largely increased. As these decorated oxide nanotubes are composed of $CN_x$ with an excellent electrical conductivity and oxide nanotubes with a typical ferromagnetic behavior, they are expected to apply in the field of electromagnetic shielding and microwave absorbing in future.

## Acknowledgements

This research is supported in part by Chinese National "863" fund (grant no. 2006AA03Z570), Beijing Natural Science Foundation (grant no. 2092026) and Research Startup Fund of North China Institute of Water Conservancy and Hydroelectric Power (no. 201011).

## References

[1] S. Iijima, Nature 354 (1991) 56–58.
[2] A. Vijayaraghavan, K. Kanzaki, S. Suzuki, Y. Kobayashi, H. Inokawa, Y. Ono, S. Kar, P.M. Ajayan, Nano Lett. 5 (2005) 1575–1579.
[3] S.F. Wang, L. Shen, W.D. Zhang, Y.J. Tong, Biomacromolecules 6 (2005) 3067–3072.
[4] X. Gui, J. Wei, K. Wang, A. Cao, H. Zhu, Y. Jia, Q. Shu, D. Wu, Adv. Mater. 22 (2010) 617–621.
[5] M. Terrones, P.M. Ajayan, F. Banhart, X. Blase, D.L. Carroll, J.C. Charlier, R. Czerw, B. Foley, N. Grobert, R. Kamalakaran, Appl. Phys. A 74 (2002) 355–361.
[6] M.S. He, S. Zhou, J. Zhang, Z.F. Liu, C. Robinson, J. Phys. Chem. B 109 (2005) 9275–9279.
[7] H.P. Lin, C.Y. Mou, S.B. Liu, Adv. Mater. 12 (2000) 103–106.
[8] S. Kobayshi, K. Hanabusa, N. Hamasaki, M. Kimura, H. Shirai, Chem. Mater. 12 (2000) 1523–1525.
[9] B.B. Lakshmi, P.K. Dorhout, C.R. Matrin, Chem. Mater. 9 (1997) 857–862.
[10] Y. Ono, K. Nakashima, M. Sano, J. Hojo, S. Shinkai, Chem. Commun. (1998) 1477–1478.
[11] Q. Kuang, Z.W. Lin, W. Lian, Z.Y. Jiang, Z.X. Xie, R.B. Huang, L.S. Zheng, J. Solid State Chem. 180 (2007) 1236–1242.
[12] C.S. Shi, G.Q. Wang, N.Q. Zhao, X.W. Du, J.J. Li, Chem. Phys. Lett. 454 (2008) 75–79.
[13] R. Umeda, H. Awaji, T. Nakahodo, H. Fujihara, J. Am. Chem. Soc. 130 (2008) 3240–3241.
[14] M.H. Yang, J.H. Jiang, Y.H. Lu, Y. He, G.L. Shen, R.Q. Yu, Biomaterials 28 (2007) 3408–3417.
[15] W. Lee, R. Scholz, K. Niesch, U. Gosele, Angew. Chem. Int. Ed. 44 (2005) 6050–6054.
[16] A.B.F. Martinson, J.W. Elam, J.T. Hupp, M.J. Pellin, Nano Lett. 7 (2007) 2183–2187.
[17] S.B. Lee, D.T. Mitchell, L. Trofin, T.K. Nevanen, H. Soderlund, C.R. Martin, Science 296 (2002) 2198–2200.
[18] Y.H. Wu, P.W. Qiao, J.J. Qiu, T.C. Chong, Nano Lett. 2 (2002) 161–164.
[19] P.C.P. Watts, W.K. Hsu, D.P. Randall, V. Kotzeva, G.Z. Chen, Chem. Mater. 14 (2002) 4505–4508.
[20] K.C. Chin, A. Gohel, W. Ji, G.L. Chong, K.Y. Lim, Chem. Phys. Lett. 383 (2004) 72–75.
[21] D. Shi, J.P. Cheng, F. Liu, X.B. Zhang, J. Alloys Compd. 502 (2010) 365–370.
[22] T. Kim, G.A. Nunnery, K. Jacob, J. Schwartz, X.T. Liu, R. Tannenbaum, J. Phys. Chem. C 114 (2010) 6944–6951.
[23] W.T. Wang, Q.L. Li, C.B. Chang, Synth. Met. 161 (2011) 44–50.
[24] A.V. Ellis, K. Vijayamohanan, R. Goswami, N. Chakrapani, L.S. Ramanathan, P.M. Ajayan, G. Ramanath, Nano Lett. 3 (2003) 279–282.
[25] K.Y. Jiang, A. Eitan, L.S. Schadler, P.M. Ajayan, R.W. Siegel, N. Grobert, M. Mayne, M. Reyes-Reyes, H. Terrones, M. Terrones, Nano Lett. 3 (2003) 275–277.
[26] X. Lepró, E. Terrés, Y. Vega-Cantú, F.J. Rodríguez-Macías, H. Muramatsu, Y.A. Kim, T. Hayahsi, M. Endo, M. Terrones, Chem. Phys. Lett. 463 (2008) 124–129.
[27] W.W. Li, C. Gao, H.F. Qian, J.C. Ren, D.Y. Yan, J. Mater. Chem. 16 (2006) 1852–1859.
[28] S. Kim, H.R. Lee, Y.J. Yun, S. Ji, K. Yoo, W.S. Yun, J.Y. Koo, D.H. Ha, Appl. Phys. Lett. 91 (2007) 093126.
[29] A. Oki, L. Adams, V. Khabashesku, Y. Edigin, P. Iney, Z.P. Luo, Mater. Lett. 62 (2008) 918–922.
[30] N.Q. Jia, L.J. Wang, L. Liu, Q. Zhou, Z.Y. Jiang, Electrochem. Commun. 7 (2005) 349–354.
[31] H. Maruyama, S.H. Yoshimura, S.J. Akita, A. Nagataki, Y. Nakayama, J. Appl. Phys. 102 (2007) 094701.
[32] H.Y. Wu, Y. Zhao, Q.Z. Jiao, J. Alloys Compd. 487 (2009) 591–594.

[33] Y. Cao, Y. Zhao, Q.Z. Jiao, Mater. Chem. Phys. 122 (2010) 612–616.
[34] L. Liu, S.S. Fan, J. Am. Chem. Soc. 123 (2001) 11502–11503.
[35] J.T. Chen, M. Zhang, T.P. Russell, Nano Lett. 7 (2007) 183–187.
[36] M.C. Tsai, G.T. Lin, H.T. Chiu, C.Y. Lee, J. Nanopart. Res. 10 (2008) 863–869.
[37] M. Terrones, N. Grobert, H. Terrones, Carbon 40 (2002) 1665–1684.
[38] M. Glerup, M. Castignolles, M. Holzinger, G. Hug, A. Loiseau, P. Bernier, Chem. Commun. (2003) 2542–2543.
[39] F.L. Normand, J. Hommet, T. Szorenyi, C. Fuchs, E. Fogarassy, Phys. Rev. B 64 (2001) 235416–235515.